Protein Engineering, Design & Selection, 2017, vol. 30 no. 3, pp. 207–218
doi: 10.1093/protein/gzw075
Advance Access Publication Date: 10 January 2017
Original Article

OXFORD

Original Article

Ligand characterization of CYP4B1 isoforms modified for high-level expression in *Escherichia coli* and HepG2 cells

Katharina Roellecke[1], Vera D. Jäger[2], Veselin H. Gyurov[2], John P. Kowalski[3], Stephanie Mielke[2], Allan E. Rettie[3], Helmut Hanenberg[1,4], Constanze Wiek[1,†*], and Marco Girhard[2,†*]

[1]Department of Otorhinolaryngology and Head/Neck Surgery, Heinrich-Heine University, 40225 Düsseldorf, Germany, [2]Institute of Biochemistry, Heinrich-Heine University, 40225 Düsseldorf, Germany, [3]Department of Medicinal Chemistry, School of Pharmacy, University of Washington, Seattle, WA 98195, USA, and [4]Department of Pediatrics III, University Children's Hospital Essen, University of Duisburg-Essen, 45122 Essen, Germany

[*]To whom correspondence should be addressed. E-mail: constanze.wiek@med.uni-duesseldorf.de (C.W.); marco.girhard@hhu.de (M.G.)
[†]These authors contributed equally.
Edited by Dagmar Ringe

Received 28 September 2016; Revised 5 December 2016; Editorial Decision 6 December 2016; Accepted 6 December 2016

Abstract

Human CYP4B1, a cytochrome P450 monooxygenase predominantly expressed in the lung, inefficiently metabolizes classical CYP4B1 substrates, such as the naturally occurring furan pro-toxin 4-ipomeanol (4-IPO). Highly active animal forms of the enzyme convert 4-IPO to reactive alkylating metabolite(s) that bind(s) to cellular macromolecules. By substitution of 13 amino acids, we restored the enzymatic activity of human CYP4B1 toward 4-IPO and this modified cDNA is potentially valuable as a suicide gene for adoptive T-cell therapies. In order to find novel pro-toxins, we tested numerous furan analogs in *in vitro* cell culture cytotoxicity assays by expressing the wild-type rabbit and variants of human CYP4B1 in human liver-derived HepG2 cells. To evaluate the CYP4B1 substrate specificities and furan analog catalysis, we optimized the N-terminal sequence of the CYP4B1 variants by modification/truncation and established their heterologous expression in *Escherichia coli* (yielding 70 and 800 nmol·l^{-1} of recombinant human and rabbit enzyme, respectively). Finally, spectral binding affinities and oxidative metabolism of the furan analogs by the purified recombinant CYP4B1 variants were analyzed: the naturally occurring perilla ketone was found to be the tightest binder to CYP4B1, but also the analog that was most extensively metabolized by oxidative processes to numerous non-reactive reaction products.

Key words: CYP4B1, cytochrome P450 monooxygenase, 4-ipomeanol, perilla ketone, suicide gene

Introduction

In mammalian species, cytochromes P450 are monooxygenases that are responsible for the metabolism of endogenous and also exogenous chemicals (Hasler *et al.*, 1999). However, unlike other members of CYP4, the sub-family CYP4B1 not only has the capacity to ω-hydroxylate medium chain fatty acids (MCFAs) but also to metabolize protoxic xenobiotics which are chemically unrelated (Baer and Rettie, 2006; Zhang *et al.*, 2006; Edson and Rettie, 2013). One of these xenobiotics is 4-ipomeanol (4-IPO) **12**; a substance produced by *Ipomea batatas* as defense mechanism when infected with the

common mold *Fusarium solani*. Since CYP4B1 is predominantly expressed in lung Clara cells and Type II pneumocytes, feeding livestock with mold-infected sweet potatoes has led to severe respiratory distress and death. Based on the tissue distribution of CYP4B1, the specific lung toxicity caused by 4-IPO **12**, and the 4-IPO-sensitivity of some human non-small cell lung cancer cell lines (Falzon *et al.*, 1986), 4-IPO **12** was tested as an anti-cancer drug in three clinical Phase I/II studies (Rowinsky *et al.*, 1993; Kasturi *et al.*, 1998; Lakhanpal *et al.*, 2001). However, despite the pre-clinical data, none of the clinical studies showed any anti-tumor activity or lung toxicity.

The alignment of different xenobiotic-metabolizing P450 protein sequences revealed a conserved proline residue in the meander region which is located two amino acids N-terminal to the distal arginine of the putative 'ERR triad' that is important for heme binding. In wild-type human CYP4B1, this conserved proline should be located at position 427, but is replaced by serine (Zheng *et al.*, 1998) that renders the human enzyme incapable of processing 4-IPO **12** (Baer *et al.*, 2005). Therefore, as humans cannot process 4-IPO **12**, Rainov *et al.* (1998) proposed to use the rabbit CYB4B1 as a suicide gene in combination with 4-IPO **12** as pro-drug to treat brain tumors. This suicide gene system approach would require that the tumor cells *in vivo* in patients be equipped with the rabbit *CYP4B1* cDNA, e.g. injection of infectious viral particles into the tumors. The transduced tumor cells could then be selectively killed after 4-IPO **12** infusion, as the encoded protein converts the non-toxic substance into a cell toxin. However, it has not been technically possible to efficiently target the vast majority of brain tumor cells (Rainov, 2000), which is necessary for meaningful anti-tumor effects.

Suicide genes are still an important tool for *in vivo* safety control in adoptive cellular immunotherapy with autologous or allogeneic T-cells genetically modified with chimeric antigen receptors or affinity-enhanced T-cell receptor chains (reviewed in Karjoo *et al.* (2016)). The concept of using the human CYB4B1 as a suicide gene was developed by Wiek *et al.* (2015) who showed that the exchange p.S427P (h-P427) is important for both protein stability as well as partially rescuing the catalytic activity of the human enzyme against 4-IPO **12**. In contrast, the exchange p.P422S in rabbit CYP4B1 (r-S422) was not essential for catalytic activity against 4-IPO **12** (Wiek *et al.*, 2015), thus suggesting that additional amino acids in the rabbit protein are responsible for the high enzymatic activity toward 4-IPO **12**. An extended systematic screen identified additional 12 amino acids in the wild-type r-P422 that were key for conferring the high 4-IPO **12** metabolizing activity of this enzyme to the variant h-P427 (Wiek *et al.*, 2015). Introduction of these 12 alterations into h-P427 resulted in the h-P + 12 enzyme (R124K/E130D/L135F/V156I/T158A/E159D/E170K/N190D/R199K/T202S/D217E/L226I/S427P) that was as stable and as active against 4-IPO **12** as r-P422 when introduced into human liver cells or in primary human T-cells (Wiek *et al.*, 2015). Moreover, in perilla ketone (PK) **13**, which is present in the essential oil of *Perilla frutescens* and induced severe pulmonary toxicity in laboratory animals and livestock (Boyd, 1976; Breeze *et al.*, 1984; Garst *et al.*, 1985; Kerr *et al.*, 1986), we identified a novel substrate for the CYP4B1 suicide gene that induces a stronger toxicity in primary human T-cells than 4-IPO **12** (Roellecke *et al.*, 2016).

Although the re-engineered human CYP4B1 (h-P + 12) is generally suitable as a suicide gene, little is known about the biochemical properties of the protein itself. One interesting feature of the CYP4 family is that the P450s belonging to this family covalently bind their heme groups via an ester link between heme and a carboxylic acid (Henne *et al.*, 2001b; Ortiz De Montellano, 2008). In CYP4B1, this ester link is formed via the conserved I-helix residue Glu310 (Zheng *et al.*, 2003). Cheesman *et al.* (2003) were able to modify the N-terminus of the r-P422 enzyme for high-level expression in *Escherichia coli* and purification of the recombinant protein; in addition, they demonstrated that this recombinant enzyme also has 98% of its heme covalently bound. Using the purified recombinant rabbit enzyme, Baer *et al.* (2005) identified the bioactivation pathway for 4-IPO **12** using *N*-acetyl cysteine (NAC) and *N*-acetyl lysine (NAL) as exogenous nucleophiles to trap the formed reactive 4-IPO enedial intermediate *in vitro*. However, neither the mechanism *in vivo* nor the endogenous substrate(s) and function(s) of CYP4B1 are known to date.

In this study, we identified several new furan substrates for CYP4B1 with regard to their potential as cytotoxic pro-drugs and describe for the first time the recombinant expression of active human CYP4B1 isoforms in *E. coli*. Finally, we used the recombinant enzymes to compare their spectral binding interactions and oxidative metabolism toward a variety of different substrates.

Materials and methods

Plasmid construction

The rabbit *CYP4B1* cDNA (GenBank NM_001082103, isoform 1) cloned into expression vector pCWOri (construct 4B1#7) and the human *CYP4B1* cDNA (GenBank NM_000779, transcript variant 2) were obtained as described previously (Zheng *et al.*, 1998; Cheesman *et al.*, 2003).

Human *CYP4B1* cDNA optimized for human codon usage according to our design was bought from Geneart (Regensburg, Germany) (Wiek *et al.*, 2015). All lentiviral vectors were generated as described previously (Wiek *et al.*, 2015; Roellecke *et al.*, 2016).

The non-codon-optimized human *CYP4B1* variant h-P + 12 was obtained as cDNA gene from Eurofins Genomics (Germany), while genes codon optimized for expression in *E. coli* were bought from GenScript (*coop h-S427Δ2* and *coop r-P422Δ2*, USA). For high-level expression in *E. coli*, the expression vectors pET-22b(+) (Novagen, Germany) and pCWOri (Barnes, 1996) were used. *CYP4B1* genes were PCR-amplified and cloned into the expression vectors as described in detail in the Supplementary Methods. The oligonucleotides are listed in the Supplementary Tables S1 and S2. All genes for expression in *E. coli* contained a C-terminal His_6-tag for purification.

Cells and bacteria

Human liver cancer cells (HepG2) were purchased from ATCC (USA) and grown in Dulbecco's modified Eagle's medium GlutaMAX supplemented with 10% fetal bovine serum, 100 $U \cdot ml^{-1}$ penicillin and 100 $\mu g \cdot ml^{-1}$ streptomycin (all from Gibco Lifescience, Thermo Fischer Scientific, USA).

Escherichia coli K12 and DH5α (New England Biolabs, Germany) were used for cloning purposes, while *E. coli* DH5α F'I^q ([*F´ proA*$^+$*B*$^+$ *lacI*^{q} *Δ(lacZ)M15 zzf::Tn10* (Tet^R)/*fhuA2Δ(argF-lacZ)U169 phoA glnV44 Φ80Δ(lacZ)M15 gyrA96 recA1 relA1 endA1 thi-1 hsdR17*]; New England Biolabs, Germany) and *E. coli* OverExpress C43(DE3) ([F$^-$ *ompT hsdS*$_B$ (*r*$_B^-$ *m*$_B^-$) *gal dcm* (DE3)]; Lucigen Corporation, USA) were employed for protein expression.

Chemicals and enzymes

A library containing target compounds **1–20** was set up (Fig. 1). 4-IPO **12** was obtained from the Drug Synthesis and Chemistry Branch, National Cancer Institute (Bethesda, MD). PK **13** was

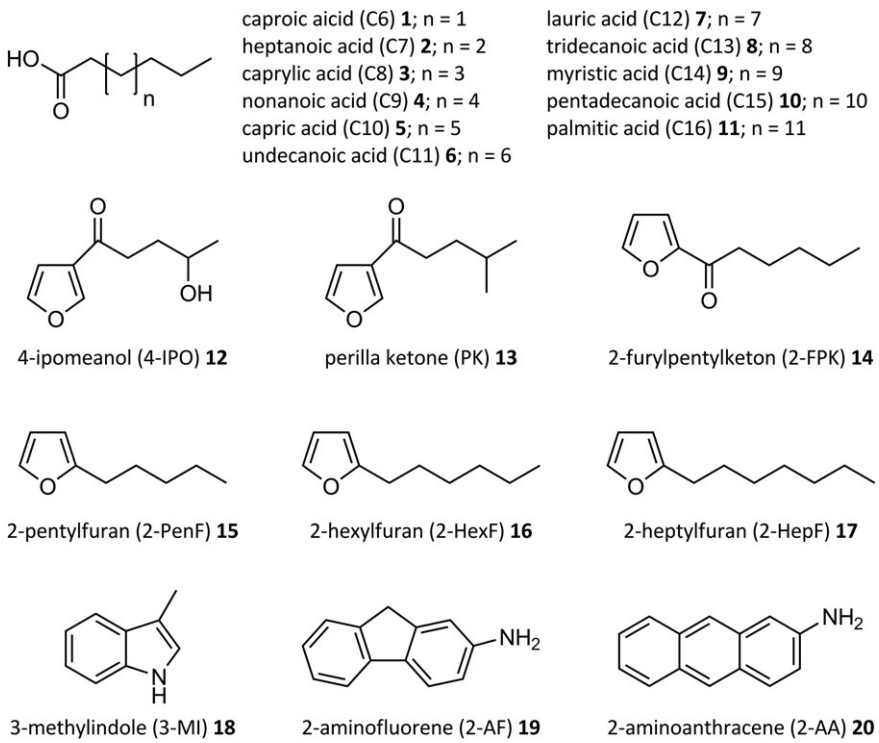

Fig. 1 Target compounds investigated with CYP4B1 isoforms. Compounds **12–20** were used in survival assays with HepG2 cells; compounds **1-20** were used to determine K_D values and/or *in vitro* conversions.

synthesized and purified according to a previously published method (Matsuura, 1957). *n*-Pentyl 2-furyl ketone (2-FPK) **14**, 2-*n*-pentylfuran (2-PenF) **15**, 2-*n*-hexylfuran (2-HexF) **16**, 2-*n*-heptylfuran (2-HepF) **17**, 3-methylindole (3-MI) **18**, 2-aminofluorene (2-AF) **19** and 2-aminoanthracene (2-AA) **20**, as well as fatty acids **1–11** and (–)-carvone were purchased from Sigma-Aldrich (Germany). Catalase from bovine liver and human CPR (recombinantly expressed in baculovirus infected insect cells) were also obtained from Sigma-Aldrich.

Cell proliferation assay and FACS analysis

Cytotoxic effects of the compounds **12–18** were evaluated using a cell proliferation assay as described previously (Schmidt *et al.*, 2015; Wiek *et al.*, 2015). Briefly, HepG2 cells were lentiviraly transduced, seeded in a 12-well plate and incubated with increasing concentrations (2.9–900 µM) of the substrates. After 24 and 48 h, cells were harvested, stained with propidium iodide for live/dead cell discrimination and analyzed by flow cytometry on a FACSCalibur (BD Biosciences, Germany).

Expression of CYP4B1 enzymes and glucose dehydrogenase in *E. coli*

While *CYP4B1* cDNAs cloned into pET-22b(+) were expressed exclusively with *E. coli* C43(DE3), expression of *CYP4B1* cloned into pCWOri was performed either in strain DH5α F'I^q or in C43 (DE3).

The general procedure followed a protocol established previously for r-P422 (Cheesman *et al.*, 2003). Briefly, cultures were grown in 400 ml TB medium supplemented with 100 µg·ml^{-1} ampicillin, 1 mM thiamine and 400 µl trace element solution (27 g·l^{-1} $FeCl_3{\cdot}6H_2O$, 2.0 g·L^{-1} $ZnCl_2{\cdot}4H_2O$, 2.0 g·l^{-1} $CoCl_2{\cdot}6H_2O$, 2.0 g·l^{-1} $Na_2MoO_4{\cdot}2H_2O$, 2.0 g·l^{-1} $CaCl{\cdot}2H_2O$, 1.0 g·l^{-1} $CuCl_2$, 0.5 g·l^{-1} H_3BO_3, 100 ml·l^{-1} of 37% HCl). The initial OD_{600}, temperature and shaking speed were adjusted to 0.03, 37°C and 180 r.p.m., respectively. When OD_{600} reached 0.4, 500 µM 5-aminolevulinic acid and isopropyl β-D-1-thiogalactopyranoside, 1 mM for pCWOri or 250 µM for pET-22b(+) expression, were added and the culture conditions changed to 27°C, 120 r.p.m. for 48 h. Cells were harvested by centrifugation (5000 × *g*, 4°C, 10 min) and the pellets were frozen at −20°C until further use.

Glucose dehydrogenase (GDH) from *Bacillus megaterium* (*gdhIV*; GenBank D10626) was expressed by pET-22b(+) in *E. coli* BL21(DE3) as described previously (Khatri *et al.*, 2015).

Purification of CYP4B1 and determination of protein concentrations

Cell pellets were resuspended in 25 ml resuspension buffer (50 mM KPi, pH 7.4, 10% glycerol, 0.5% Igepal CO-520, 0.1% dimethyl sulfoxide (DMSO), 20 mM β-mercaptoethanol, 500 mM KCl). Protease inhibitors were added as follows: 1 ml solution of 'cOmplete^{TM} EDTA-free protease inhibitor cocktail tablets' (Roche Diagnostics, Germany) if strain DH5α F'I^q was used for expression or 200 µM phenylmethylsulfonyl fluoride for strain C43(DE3).

Cells were disrupted on a High-pressure Cell Disruptor (Benchtop model TS 1.1, Constant Systems Limited, UK) with two cycles at 1.9 kbar. Insoluble protein and unbroken cells were removed by centrifugation at 50 000 × *g*, 4°C, 30 min and the supernatant (soluble protein fraction) was recovered and filtered (0.45 µm diameter).

For purification by affinity chromatography, the supernatant was loaded onto a HisTrap excel column (2 × 5 ml column volume; GE Healthcare, Germany) that was equilibrated with purification buffer

(50 mM KPi, pH 7.4, 10% glycerol, 500 mM KCl). The washing step contained 40 mM imidazole in purification buffer, while bound CYP4B1 was eluted with 200 mM imidazole in purification buffer. Desalting and removal of detergent and imidazole was achieved by application of a PD MidiTrap G-25 column (GE Healthcare) that was equilibrated with storage buffer (50 mM KPi, pH 7.4, 10% glycerol, 500 µM EDTA). Purified CYP4B1 was concentrated by ultrafiltration (30 kDa molecular weight cut-off) and aliquots were stored at −20°C until further use.

Protein concentrations were estimated by the Bradford protein assay (Bradford, 1976). CYP4B1 concentrations of non-purified enzymes were determined by the CO-difference spectral assay with $\varepsilon_{450-490}$ = 91 $mM^{-1}{\cdot}cm^{-1}$ (Omura and Sato, 1964). CO-difference spectra of purified CYP4B1 preparations were measured according to an optimized method described previously (Zheng *et al.*, 2003).

Determination of spectral dissociation constants

Spectral dissociation constants were determined as described previously (Girhard *et al.*, 2010; Khatri *et al.*, 2010). A double beam UV/VIS spectrometer (Lambda 35, PerkinElmer, Germany) was equipped with two tandem quartz cuvettes (Hellma, Germany). One chamber of each cuvette contained 1 µM CYP4B1 in buffer (50 mM KPi, pH 7.5), while the second chamber contained buffer alone. Target compounds **1–20** were titrated in small aliquots (0.5–2 µl) of an appropriate stock solution in DMSO or ethanol into the P450 containing chamber of the sample cuvette and the buffer containing chamber of the reference cuvette. The difference spectra of spectral changes between 350 and 500 nm were then recorded. Utilizing this method, contributions from turbidity or from the spectrum of the ligand can be lowered considerably (Jefcoate, 1978).

Spectral dissociation constants (K_D) were calculated by plotting the peak-to-trough difference in absorbance (ΔA) against the concentration of the ligand (L) and fitting the data to a hyperbolic equation, where ΔA_{max} is the maximum absorbance difference extrapolated to infinite ligand concentration.

$$\Delta A = \frac{\Delta A_{max}(L)}{K_D + (L)}.$$

Because of the high binding affinities of ligands **13–19** (K_D within fivefold of the P450 concentration (E)), a nonlinear regression analysis using a quadratic equation for tight binding according to Greco and Hakala (1979) was applied to determine K_D for these ligands.

$$\Delta A = \frac{\Delta A_{max}}{2(E)} \times \left\{ \left[K_D + (E) + (L)\right] - \left[\left[K_D + (E) + (L)\right]^2 - 4(E)(L)\right]^{1/2} \right\}.$$

Substrate depletion by CYP4B1 and quantitative GC/MS analysis

Substrate depletion by purified CYP4B1 isoforms was assayed by quantitative GC/MS. The activity of CYP4B1 was reconstituted *in vitro* with human cytochrome P450 reductase (CPR) and an NADPH regeneration system consisting of D-glucose and GDH from *B. megaterium* was applied.

Reaction mixtures were set up in 50 mM KPi, pH 7.5 in a total volume of 150 µl containing 0.75 µM CYP4B1, 1.5 µM CPR, 90 U catalase (for scavenging H_2O_2), 20 mM D-glucose; 2.5 U GDH, 200 µM of a target compound (300 µM in case of PK **13**) and 200 µM NADPH. The reaction mixtures were incubated at 30°C for 0.5–2 h. Negative controls did not contain CYP4B1 and CPR.

After the desired reaction time, samples containing lauric acid (C12) **7** were prepared for GC/MS analysis by addition of 5 µl of 37% HCl and extracted twice with 500 µl diethyl ether (Khatri *et al.*, 2015). All other target compounds were extracted with 200 µl ethyl acetate.

For quantitative determination of a target compound, the response of the MS-detector was calibrated by addition of 50 µM of an internal standard (ISTD) immediately before extraction of a sample: 2-HexF **16** in cases of PK **13** and 2-HepF **17**; (–)-carvone in cases of 4-IPO **12**, 2-FPK **14**, 2-HexF **16**, 3-MI **18** and 2-AF **19**.

GC/MS analysis was carried out on a GC/MS QP2010 (Shimadzu, Japan), equipped with an FS-Supreme-5 column (30 m × 0.25 mm × 0.25 µm; Chromatographie Service GmbH, Germany). Helium was used as carrier gas and the linear velocity was set to 30 $cm{\cdot}min^{-1}$.

Analysis of C12 **7** conversions and identification of conversion products was performed as described previously (Khatri *et al.*, 2015). For analysis of target compounds 4-IPO **12**, PK **13**, 2-FPK **14**, 2-HexF **16** and 2-HepF **17**, the column temperature was maintained at 70°C for 2 min, ramped to 220°C with a rate of 10°C·min^{-1}, then to 300°C at a rate of 40°C·min^{-1}, and held at 300°C for 1 min. For 3-MI **18**, the temperature program was as follows: 110°C for 2 min, ramp to 250°C at a rate of 10°C·min^{-1}, hold for 1 min, then to 300°C at a rate of 25°C·min^{-1}, hold for 1 min. For 2-AF **19**, the column temperature was maintained at 110°C for 2 min, increased to 300°C at a rate of 10°C·min^{-1}, and held for 3 min.

Identification of PK and 4-IPO metabolites by UPLC

Reconstituted systems of 0.75 µM purified P450, 1.5 µM CPR, 3 µg 1,2-didodecanoyl-sn-glycero-3-phosphocholine and 90 U catalase in 50 mM KPi, pH 7.4 were set up in a total volume of 150 µl. 4-IPO **12** or PK **13** was then added to a final concentration of 200 µM (using 20 mM stock solutions in methanol). Metabolism was initiated via addition of NADPH (1 mM final concentration), and incubations progressed at 37°C for 30 min. Reactions were terminated by the addition of 20 µl of a 15% zinc sulfate solution. Supernatant (10 µl) was analyzed by UPLC utilizing a HSS T3 column (1.8 µm × 2.1 × 100 mm). Initial conditions were 95% solution A (0.1% formic acid in H_2O) and 5% solution B (0.1% formic acid in acetonitrile) at a flow rate of 0.3 ml·min^{-1}.

For analysis of PK **13** metabolism, the linear gradient increased B from 5 to 90% between 0 and 20 min, followed by a 3 min isocratic period; the total run time was 28 min. For analysis of 4-IPO **12** metabolism, the linear gradient increased B from 5 to 17% between 0 and 20 min, 17–90% between 20 and 23 min, followed by a 2 min isocratic period; the total run time was 28 min.

UPLC-UV detection was performed on a Waters Acquity instrument UPLC system paired with a Waters Acquity Photodiode Array (PDA) eλ Detector. UV analysis was performed at a wavelength of 254 nm, and data were collected using Empower 3 Software. UPLC-MS detection was performed on a Thermo Linear Trap Quadrupole Orbitrap coupled to a Waters Acquity UPLC System. The mass spectrometer was run in ESI+ mode, and data analysis was performed using Xcalibur.

Results

We and others have demonstrated the efficiency of the CYP4B1/4-IPO suicide gene system in human cells, either with the rabbit isoform r-P422 (Rainov *et al.*, 1998; Mohr *et al.*, 2000) or with the re-engineered human isoform h-P + 12 (Schmidt *et al.*, 2015; Wiek *et al.*, 2015; Roellecke *et al.*, 2016). Since an endogenous substrate

for any of the CYP4B1 isoforms is unknown and in order to better understand potential endogenous functions and also to find new cytotoxic pro-drugs, we created a library of potential substrates shown in Fig. 1. Compounds **1–11** were chosen because fatty acids with chain length C7–C12 are known to be processed by r-P422 (Fisher *et al.*, 1998). Among other known substrates for CYP4B1 enzymes are several pro-toxins, including 4-IPO **12** (Verschoyle *et al.*, 1993; Smith *et al.*, 1995), 3-MI **18** (Ramakanth *et al.*, 1994; Thornton-Manning *et al.*, 1996), 2-AF **19** (Robertson *et al.*, 1983; Vanderslice *et al.*, 1985) and 2-AA **20** (Robertson *et al.*, 1983; Smith *et al.*, 1995). The furan analogs **13–17** were chosen because of their structural similarity to 4-IPO **12**.

Cytotoxicity assay in human cells

To provide an appropriate cellular environment, the hepatic cancer cell line HepG2 was lentivirally transduced with r-P422 and three different codon-optimized human isoforms; h-S427 (endogenous wild-type protein), h-P427 (serine-to-proline exchange at position 427) and h-P + 12 (re-engineered protein established as human suicide gene (Wiek *et al.*, 2015)). EGFP co-expressed via an internal ribosomal entry site (IRES) was used as a marker gene to identify transduced cells in mixed cultures (Fig. 2A). As shown before (Schmidt *et al.*, 2015; Wiek *et al.*, 2015; Roellecke *et al.*, 2016), incubation with 4-IPO **12** induced no toxicity in non- and control-transduced cells, but high toxicity in r-P422 and h-P + 12 and less toxicity in h-P427 expressing cells. After 48 h at 290 µM, only 3.3 ± 0.3% r-P422 positive cells and 8.6 ± 1.1% h-P + 12 positive cells were still viable (Fig. 2B). A similar toxicity pattern was observed with PK **13**, although less h-P427 positive cells were viable after 48 h at the different PK **13** concentrations, when compared with 4-IPO **12** (e.g. at 290 µM 10.9 ± 1.9% vs. 32.1 ± 2.3% viable cells; Fig. 2C). Surprisingly, incubation with 2-FPK **14**—with a similar structure as 4-IPO **12** and PK **13**—led to clear toxicity in r-P422 expressing cells but resulted in relatively low cytotoxic activities in h-P427 and h-P + 12 positive cells (48 h at 290 µM: 69.6 ± 3.2% vs. 81.5 ± 5.7% viable cells; Fig. 2D). Similarly, compounds 2-PenF **15** and 2-HexF **16**, both harboring a furan ring with carbon side chains of different length, led to major toxicity in r-P422 positive cells, while HepG2 cells stably expressing the three human isoforms were relatively little affected (Fig. 2E and F). In contrast, the very similar 2-HepF **17** exhibited cytotoxicity only at high substrate concentrations in all cells regardless whether a CYP4B1 isoform was expressed or not (Fig. 2G); therefore, this is considered unspecific toxicity/cell death.

3-MI **18**, known to cause pulmonary toxicity in livestock (Yost, 1989), induced unspecific toxicity in all cells already at 29 µM, although cells expressing r-P422, h-P + 12 and to a lesser extent h-P427 displayed a higher death rate (Fig. 2H) suggesting that CYP4B1 is involved in the conversion of 3-MI **18**. 2-AF **19** only induced solely unspecific cell death in all test groups at 290 µM (Fig. 2I). In contrast, 2-AA **20**, a previously proposed pro-drug for r-P422 as the suicide gene (Rainov *et al.*, 1998; Mohr *et al.*, 2000; Jang *et al.*, 2010), induced specific cytotoxicity in r-P422, h-P427 and also h-P + 12 expressing cells albeit the pro-drug activation rate seemed to be the highest with the r-P422 enzyme (8 ± 1.1% viable cells after 48 h at 290 µM; Fig. 2J).

Expression of N-terminally modified rabbit CYP4B1 in *E. coli*

In order to express rabbit CYP4B1 in *E. coli*, we used either an N-terminal truncation of amino acids 2–19 with the second codon changed to Alanine—MA (r-P422Δ1), or the Barnes sequence—MALLLAVF (r-P422Δ2) (Barnes *et al.*, 1991). After high-pressure cell disruption and addition of a detergent for solubilization, the presence of spectrally intact CYP4B1 was verified by recording reduced CO-difference spectra with a maximum near 450 nm (Supplementary Figure S1). When the one-step cell lysis procedure was applied to r-P422Δ2, the level of soluble and active rabbit CYP4B1 was slightly lower, but still comparable to that achieved previously using a multiple-step lysozyme/sonication procedure (220 nmol·l^{-1} vs. 250 nmol·l^{-1} (Cheesman *et al.*, 2003); Supplementary Table S3). Re-solubilization of the pellet after cell lysis revealed that no spectrally active P450 remained in the insoluble fraction, demonstrating that the extraction conditions used were effective. Therefore, the one-step cell lysis procedure was used for all recombinant CYP4B1 preparations in this study.

Codon optimization for heterologous expression of genes in unrelated hosts has proven to enhance the yields of some mammalian P450s in *E. coli* (Wu *et al.*, 2009). However, expression of codon-optimized cDNA *coop r-P422Δ1* and *coop r-P422Δ2* did not lead to increased amounts of spectrally active rabbit CYP4B1 (30–50% in comparison to non-codon optimized cDNA; Supplementary Figure S1 and Table S3).

It has previously been reported that the S427 sequence modification renders the wild-type human CYP4B1 unable to bind the catalytically active heme and therefore this enzyme could not be expressed in functional form in human and insect cells (Zheng *et al.*, 1998), or in the yeast *S. cerevisiae* (Imaoka *et al.*, 2001). Reversion of the serine to the conserved proline (S427P) conferred the ability to obtain a reduced CO-difference spectrum with h-P427 (Zheng *et al.*, 1998). Likewise, a serine should also render CYP4B1 isoforms non-functional when expressed in *E. coli*. To confirm this hypothesis, the proline residue 422 in the wild-type rabbit CYP4B1 (r-P422Δ1) was exchanged to serine (r-S422Δ1). As expected, no spectrally intact P450 could be expressed in *E. coli* in this case (Supplementary Table S3), while in comparison, r-P422Δ1 yielded 195 nmol·l^{-1} of soluble and spectrally active P450 (Table I).

Expression of N-terminally modified human CYP4B1 isoforms in *E. coli*

In a first straightforward approach to express the activated h-P427 variant, expression vectors with the MALLLAVF-modification and MA-modification/truncation were generated (h-P427Δ1 and h-P427Δ2, respectively). Unexpectedly, however, no spectrally active P450 was detected in the soluble protein fractions after cell lysis. Therefore, we investigated whether other truncations of the N-terminal amino acids (h-P427Δ3-Δ7; Supplementary Table S3) would be more effective. Indeed, 20 nmol·l^{-1} of soluble and spectrally active h-P427 could be expressed when h-P427Δ3 was employed with N-terminal deletion of amino acids 2–27 (Table I and Supplementary Figure S1). The expression level of h-P427Δ3 could further be increased to 50 nmol·l^{-1} when strain *E. coli* C43 (DE3) was used instead of DH5α F'I^q (Table I).

To confirm the reports of the impact of serine on recombinant expression, the Δ3-truncation as well as the MALLLAVF-modification and MA-modification/truncation were transferred to the human wild-type *h-S427* cDNA. As expected, no spectrally active P450 was detected after recombinant expression in the soluble protein fractions by CO-difference spectral analysis (Supplementary Table S3).

Next, the Δ3-truncation was introduced in the *h-P + 12* cDNA and then cloned into the expression vector pCWOri (h-P + 12Δ3).

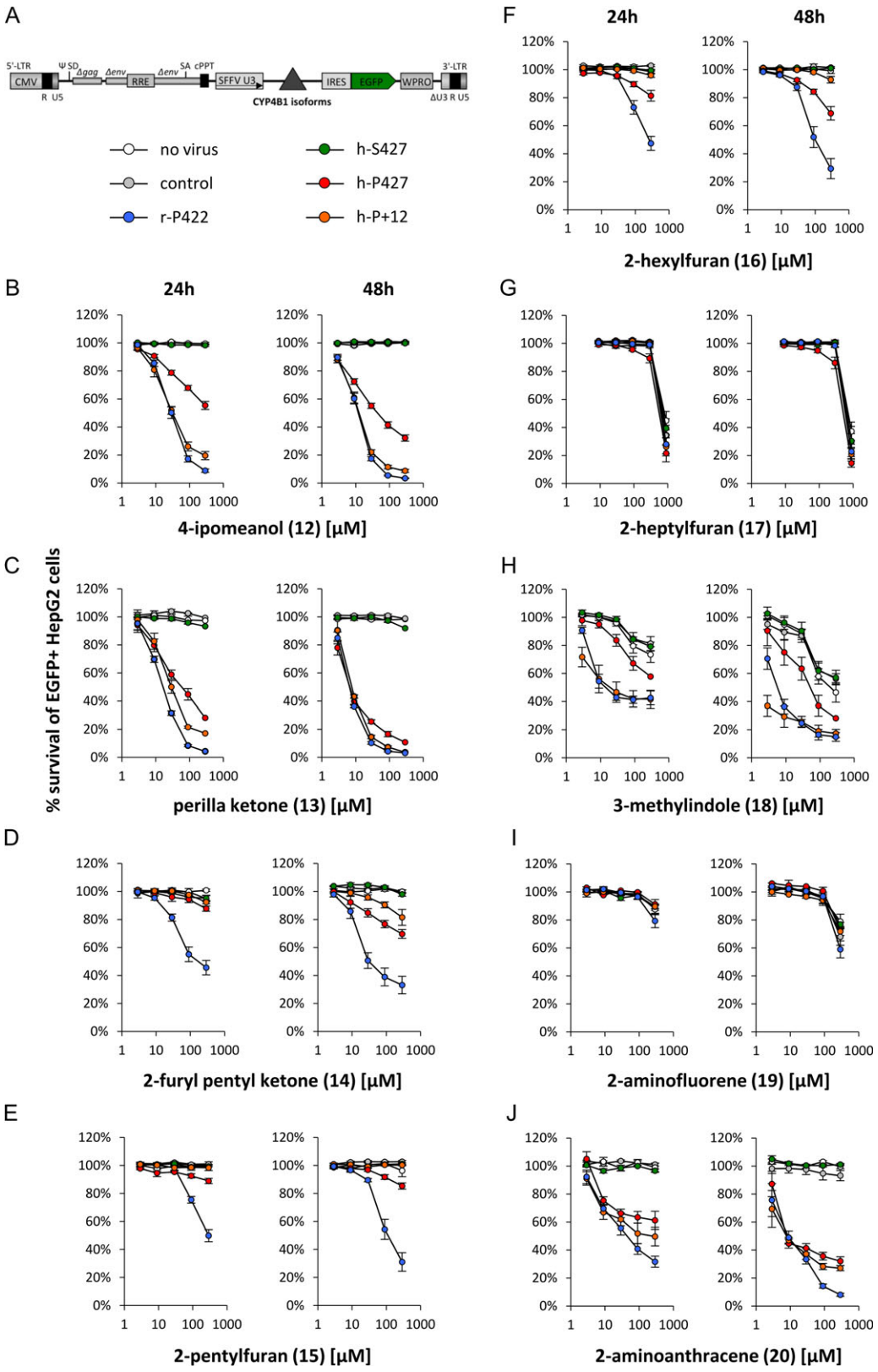

Fig. 2 Survival assay of HepG2 cells expressing different isoforms of CYP4B1. (**A**) Schematic outline of the lentiviral vector used. CYP4B1 isoforms were driven by the *spleen focus-forming virus* U3 promoter and co-expressed with EGFP via an IRES. For the assay, cells were challenged with increasing concentrations of 4-IPO **12** (**B**), PK **13** (**C**), 2-FPK **14** (**D**), 2-PenF **15** (**E**), 2-HexF **16** (**F**), 2-HepF **17** (**G**), 3-MI **18** (**H**), 2-AF **19** (**I**) or 2-AA **20** (**J**). As control vector, puc2CL6IEGwo was used. Survival was assessed after 24 and 48 h by PI staining and FACS analysis. The mean ± SEM of at least three independent experiments is shown.

Table I. Rabbit and human CYP4B1 expression in *E. coli*

Construct	Variant[a]	N-terminal sequence	C-terminal sequence	Vector	Host strain	Expression (nmol·l^{-1})[b]
r-wild-type	—	MLGFLSRLGLWASGLILILGFLKLLRLLLR	LGPKAEK*	pCWOri	DH5αF'I^q	0
r-P422Δ1	—	MA----------GFLKLLRLLLR	LGPKAEKSTHHHHHHH*	pCWOri	DH5αF'I^q	195
					C43(DE3)	570
r-P422Δ1_pET	—		LGPKAEKKLAAALEHHHHHHH*	pET−22b	C43(DE3)	800
h-wild-type	—	MVPSFLSLSFSSLGLWASGLILVLGFLKLIHLLLR	LGPGSGK*	pCWOri	DH5αF'I^q	0
h-P427Δ3	S427P	M----------KLIHLLLR	LGPGSGKSTHHHHHHH*	pCWOri	DH5αF'I^q	20
					C43(DE3)	50
h-P427Δ3_pET	S427P		LGPGSGKKLAAALEHHHHHHH*	pET-22b	C43(DE3)	25
h-P + 12Δ3	S427P + 12	M----------KLIHLLLR	LGPGSGKSTHHHHHHH*	pCWOri	DH5αF'I^q	34
					C43(DE3)	68
h-P + 12Δ3_pET	S427P + 12		LGPGSGKKLAAALEHHHHHHH*	pET-22b	C43(DE3)	30
h-P + 12Δ1	S427P + 12	MA----------GFLKLIHLLLR	LGPGSGKSTHHHHHHH*	pCWOri	DH5αF'I^q	<10
					C43(DE3)	25
h-P + 12Δ1_pET	S427P + 12		LGPGSGKKLAAALEHHHHHHH*	pET-22b	C43(DE3)	60

Comparison of expression levels reached with plasmids pCWOri and pET-22b(+) in strains *E. coli* DH5α F'I^q and C43(DE3).
[a]S427P + 12 = R124K/E130D/L135F/V156I/T158A/E159D/E170K/N190D/R199K/T202S/D217E/L226I/S427P.
[b]Determined from CO-difference spectra of soluble protein fractions after high-pressure cell disruption; average of two to three individual experiments.

Expression of h-P + 12Δ3 in the strain DH5α F'I^q resulted in 34 nmol·l^{-1} of soluble enzyme. Similar to h-P427Δ3, the expression level was doubled to 68 nmol·l^{-1} when the strain C43(DE3) was employed (Table I and Supplementary Figure S1).

Interestingly, and in contrast to h-P427Δ1, h-P + 12Δ1 (carrying the MA-modification/truncation) could also be expressed, however, the expression levels were lower compared to those of h-P427Δ3 (Table I).

These findings demonstrated that the expression levels of recombinant CYP4B1 produced in *E. coli* strongly depend on the amino-acid sequence of the enzyme: the more similar the protein is to the wild-type rabbit CYP4B1, the higher is the expression level in *E. coli*.

Comparison of the pCWOri- and pET-expression vectors

We observed that expression of the cDNAs in the pCWOri plasmid (r-P422Δ1, h-P427Δ3, h-P + 12Δ3) in *E. coli* strain C43(DE) resulted in ~2.5-fold higher amounts of soluble CYP4B1 compared to expression in strain DH5α F'I^q (Table I). The strain C43(DE3) is a BL21(DE3) derivative that contains genetic mutations phenotypically selected for conferring tolerance to toxic proteins (according to the manufacturers' protocol).

In the next set of experiments, expression plasmids for r-P422, h-P427 and h-P + 12 were generated based on pET-22b(+); this yielded r-P422Δ1_pET, h-P427Δ3_pET and h-P + 12Δ3_pET, respectively. In addition, h-P + 12Δ1_pET was also produced. Utilizing the pET-vector with C43(DE3), the expression level of r-P422Δ1 was boosted to 800 nmol·l^{-1} of soluble and spectrally active P450, which to the best of our knowledge is the highest expression level reported for any CYP4B1 isoform so far. The expression level of h-P + 12Δ1 was increased sixfold when compared with its expression in pCWOri with strain DH5α F'I^q (Table I). Interestingly, the expression levels for h-P427Δ3 and h-P + 12Δ3 were lower when compared with those of strain C43(DE3) with plasmid pCWOri, but comparable to those achieved with pCWOri in strain DH5α F'I^q (Table I).

In summary, the rather 'unusual' combination of C43(DE3) bacteria with plasmid pCWOri yielded the highest expression level for h-P427Δ3 and h-P + 12Δ3, while this was true for the more 'adequate' combination of C43(DE3) with pET-22b(+) in cases of r-P422Δ1 and h-P + 12Δ1. The strain C43(DE3) was generally superior to DH5α F'I^q.

CO-difference spectra of purified recombinant CYP4B1 isoforms

The recombinant isoforms r-P422Δ1, h-P427Δ3 and h-P + 12Δ3 were purified by nickel affinity chromatography and extensively desalted by column chromatography and ultrafiltration to remove residual imidazol and detergent. In general, the purity of the enzymes after this procedure was >85% (judging from SDS-PAGE; Supplementary Figure S2).

The addition of carbon monoxide to the purified and sodium dithionite reduced CYP4B1 isoforms produced characteristic difference spectra (Fe^{II}-CO versus Fe^{II}) with the Soret band shifted to 451 nm, however, an additional peak on the Soret feature at ~421 nm was also visible. This latter peak was most pronounced in case of h-P427Δ3, and the spectra overall looked very similar to those observed for the non-purified proteins (Supplementary Figure S1). Using an optimized method with extra reduction by addition of methyl viologen

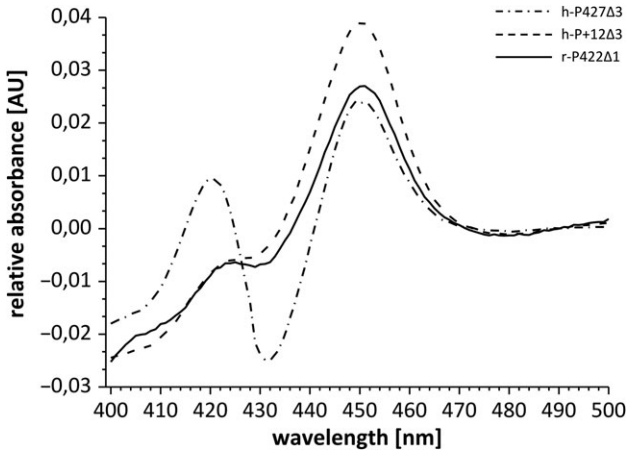

Fig. 3 CO-difference spectra of purified recombinant CYP4B1 isoforms recorded under optimized experimental conditions (Zheng *et al.*, 2003).

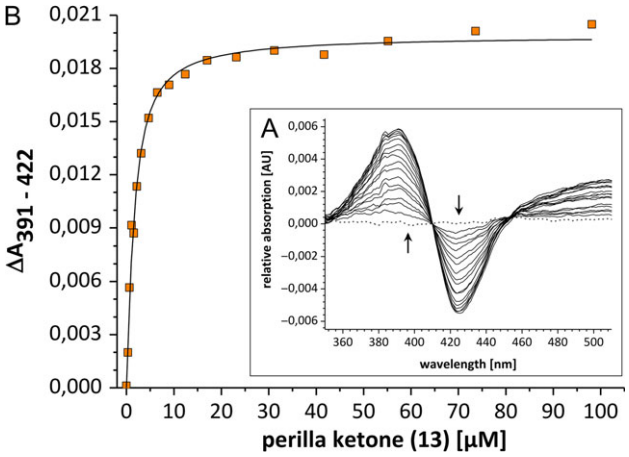

Fig. 4 Spectral binding interactions of PK and h-P + 12. (**A**) Type I spectral changes resulting from binding of PK **13** to h-P + 12Δ3; peak and trough were observed at 391 and 422 nm, respectively. (**B**) Peak-to-trough absorbance differences plotted against the respective concentration of PK **13** that was assayed. The solid line results from nonlinear regression analysis using the equation for tight binding to calculate the K_D value.

established by Zheng *et al.* (2003) to measure CO-difference spectra, nearly all of the peak at ~421 nm could be removed except for a small portion (<5%), with notable exception of h-P427Δ3 that still showed a considerable peak at ~421 nm (Fig. 3).

Determination of spectral dissociation constants

Binding of substrates and xenobiotics to P450s can result in two types of characteristic spectral changes in the UV/VIS heme Soret spectrum, referred to as Type I and Type II (Schenkman *et al.*, 1981; Isin and Guengerich, 2008). A classical Type I spectrum results from the spin-state shift of the Soret band at about 418 nm that represents the ferric (Fe^{III}) low-spin substrate free form to ~390 nm for the ferric (Fe^{III}) high-spin form originating from the displacement of H_2O as the sixth ligand when a substrate is bound in close proximity to the heme. Direct coordination of a ligand to heme iron results in a Type II spectrum characterized by a shift to 430–455 nm, but these complexes are inhibitory and generally not considered relevant to productive substrate binding leading to catalysis (Isin and Guengerich, 2008).

In this study, binding of all selected ligands to r-P422 as well as h-P427 and h-P + 12 was investigated. Generally, the addition of all compounds resulted in Type I spectral changes; this is exemplified for binding of PK **13** to h-P + 12, where peak and trough were observed at 391 and 422 nm, respectively (Fig. 4A).

The spectral binding affinities, as reflected in the dissociation constant K_D, varied considerably (Fig. 4B). For binding of fatty acids with chain lengths C6 to C16 **1–11** to r-P422 the K_D values decreased with increasing chain length, ranging from 45 ± 3 for caproic acid (C6) **1** to 6 ± 1 for pentadecanoic acid (C15) **10** (Table II). The same tendency was observed for h-P + 12 with the exception of fatty acids C11 to C13 **6–8**. When comparing r-P422 to h-P + 12, the K_D values for the MCFAs C6 to C12 **1–7** were generally higher for h-P + 12, while they were in the same range for the long chain fatty acids (LCFAs) C13 to C16 **8–11**.

The binding affinities of the furyl-containing heterocyclic aromatics **13–17** were much higher than those of the fatty acids, as represented by their ~10-fold lower K_D values in comparison to the LCFA, whereas the K_D of 4-IPO **12** was in the same range as those of the LCFA (Table II). For all CYP4B1 isoforms, very tight binding of 2-PenF **15** was observed with K_D values being in sub-micromolar range (0.06 ± 0.02 for r-P422, 0.19 ± 0.04 for h-P427 and 0.05 ± 0.01 for h-P + 12).

The K_D values for the bi- or tricyclic compounds 3-MI **18**, 2-AF **19** and 2-AA **20** that are known to be processed by r-P422 were higher than those of the furyl-containing heterocyclic aromatics **13–17** (Table II).

When comparing the binding of compounds **12–20** to different CYP4B1 isoforms, in general, the binding affinities to the human isoforms h-P427 and h-P + 12 were modestly higher when compared with that of r-P422; in most cases, the tightest ligand binding was observed for h-P427, namely with 4-IPO **12**, PK **13**, 2-HepF **17**, 3-MI **18** and 2-AF **19**.

Target compound conversion by CYP4B1 isoforms

The conversion of target compounds by CYP4B1 isoforms was assayed through substrate depletion experiments in identical *in vitro* reaction setups. The activity of recombinant r-P422, h-P427 and h-P + 12 was reconstituted with human CPR in an 1:2 ratio, and the consumption of target compounds was determined by quantitative GC/MS analysis relative to negative control reactions that did not contain recombinant CYP4B1 and CPR.

First, processing of C12 **7** by r-P422 was performed as a positive control for our reaction setup. Here, conversion of C12 **7** increased over time and after 2 h, the hydroxylated products at the ω-, ω_{-1}- and ω_{-2}-position were detected at ratios of 26:20:1 (data not shown). These data are in good accordance with published results of Cheesman *et al.* who reported a ratio of $\omega{:}\omega_{-1}$ of 3:2 for a similar *in vitro* reaction setup (Cheesman *et al.*, 2003).

In the main experiments, all tested target compounds assayed were depleted by all recombinant CYP4B1 isoforms (Table III), albeit to different extents. The highest conversion was observed for PK **13**, which reached 96.7% with r-P422 after 0.5 h (Fig. 5). This corresponds to a substrate oxidation rate (SOXR) of 8.60 $nmol{\cdot}min^{-1}{\cdot}nmol_{P450}{}^{-1}$. In comparison, PK **13** conversion by h-P427 attained only 14.1% (SOXR = 1.25), but was as high as 50.3% for the optimized h-P + 12 enzyme (SOXR = 4.47).

Table II. Substrate dissociation constants (K_D values) calculated from Type I spin-state shifts (mean ± SEM)

Type of substrate	Number (abbreviation)	K_D value (μM)		
		r-P422	h-P427	h-P + 12
MCFA	**1** (C6)	45 ± 3	63 ± 11	80 ± 11
	2 (C7)	35 ± 3	n.d.	36 ± 4
	3 (C8)	25 ± 2	n.d.	30 ± 2
	4 (C9)	23 ± 2	n.d.	21 ± 2
	5 (C10)	30 ± 4	n.d.	12 ± 1
	6 (C11)	33 ± 2	n.d.	47 ± 3
	7 (C12)	31 ± 3	40 ± 4	66 ± 3
LCFA	**8** (C13)	21 ± 4	n.d.	19 ± 2
	9 (C14)	7 ± 1	6 ± 1	5 ± 1
	10 (C15)	6 ± 1	n.d.	4 ± 1
	11 (C16)	10 ± 2	n.d.	5 ± 1
Furyl-containing heterocyclic aromatics	**12** (4-IPO)	30 ± 5	8 ± 2	28 ± 2
	13 (PK)	1.67 ± 0.82	0.25 ± 0.09	1.31 ± 0.17
	14 (2-FPK)	0.31 ± 0.05	0.68 ± 0.07	1.56 ± 0.17
	15 (2-PenF)	0.06 ± 0.02	0.19 ± 0.04	0.05 ± 0.01
	16 (2-HexF)	0.93 ± 0.10	0.51 ± 0.11	0.06 ± 0.01
	17 (2-HepF)	1.63 ± 0.41	0.09 ± 0.01	0.22 ± 0.05
Bi- or tricyclic compounds	**18** (3-MI)	2.6 ± 0.2	0.7 ± 0.2	4.9 ± 0.9
	19 (2-AF)	5.72 ± 0.17	0.79 ± 0.07	1.47 ± 0.14
	20 (2-AA)	7.6 ± 0.6	6.4 ± 0.8	6.4 ± 1.1

n.d., not determined.

Table III. Conversion of target compounds by recombinant CYP4B1 isoforms

Number (abbreviation)	Conversion r-P422		Conversion h-P427		Conversion h-P + 12	
	(μM)	(%)	(μM)	(%)	(μM)	(%)
12 (4-IPO)[a]	16.8	8.4	5.1	2.5	11.6	5.8
13 (PK)[b]	290.1	96.7	42.3	14.1	150.9	50.3
14 (2-FPK)[a]	92.6	46.3	71.8	35.9	73.2	36.6
16 (2-HexF)[a]	130.4	65.2	100.3	50.2	99.5	49.7
17 (2-HepF)[a]	114.2	57.1	116.6	58.3	113.1	56.6
18 (3-MI)[a]	21.6	10.8	18.4	9.2	28.5	14.3
19 (2-AF)[a]	8.4	4.2	7.1	3.5	3.6	1.8

[a]Determined after 2 h; 200 μM substrate concentration.
[b]Determined after 0.5 h; 300 μM substrate concentration.

The SOXR calculated for the other target compounds were considerably lower; therefore, the reaction time was prolonged to 2 h. With this prolonged incubation, the conversions of target compounds by r-P422 were generally higher compared to the two human CYP4B1 isoforms (except for 3-MI **18**); e.g. the conversions of 2-FPK **14**, 2-HexF **16** and 2-HepF **17** were in a range of 46–65% with r-P422 and 36–58% with h-P427 and h-P + 12, respectively (Table III). This is remarkable as 2-FPK **14**, 2-HexF **16** and 2-HepF **17** so far have not been reported as substrates for any CYP4B1. The lowest conversion was observed in the case of 2-AF **19** which reached a maximum of only 4.2% with r-P422 (SOXR = 0.05). This result corresponded well with the result of the cytotoxicity assay in HepG2 cells, where no effect of 2-AF **19** on cell viability was seen (Fig. 2I).

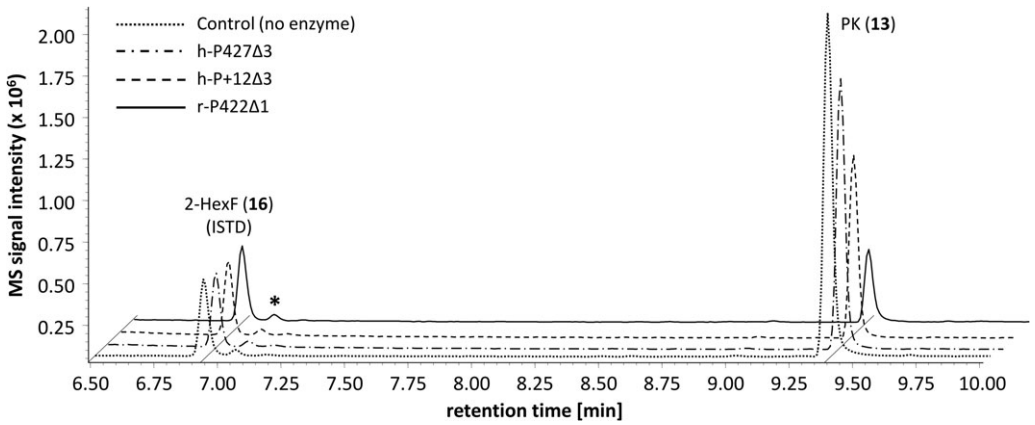

Fig. 5 GC/MS chromatograms of PK conversions by recombinant CYP4B1 enzymes. Dotted line: negative control (without addition of enzyme); dashed-dotted line: h-P427Δ3; dashed line: h-P + 12Δ3; solid line: r-P422Δ1. The small peak marked with an asterisk is an impurity that was also present in the negative control.

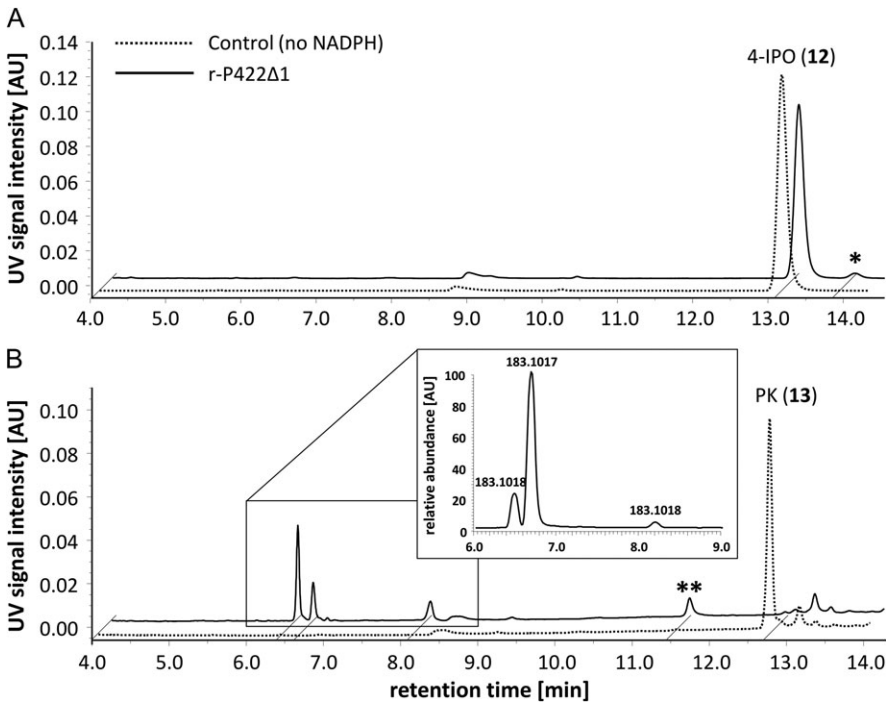

Fig. 6 UPLC chromatograms (UV detection at 254 nm) obtained for reconstituted rabbit CYP4B1 (r-P422Δ1) incubations. (**A**) 4-IPO **12** (200 μM) and (**B**) PK **13** (200 μM). Dotted line: negative control (without addition of NADPH); solid line: addition of NADPH (1 mM). The inset of (**B**) depicts a reconstructed *m/z* 183 ion chromatogram for analytes eluting between 6 and 9 min. The accurate mass measurement of 183.1017 corresponds to a hydroxylated PK-metabolite (δ p.p.m. 0.71). The small peak marked with an asterisk in case of 4-IPO **12** was tentatively identified as ipomeanine, whereas the peak marked with two asterisk in case of PK **13** represents an uncharacterized NADPH-dependent metabolite.

Identification of PK and 4-IPO metabolites

Given the very high conversion rates of the CYP4B1 enzymes for PK **13** when compared with 4-IPO **12**, we decided to identify the oxidation products generated from these two substrates by the r-P422Δ1 enzyme using HPLC-UV and UPLC-MS analysis. One minor non-reactive NADPH-dependent metabolite, tentatively identified as ipomeanine (Chen *et al.*, 2006), was formed from 4-IPO **12** under the incubation conditions (Fig. 6A). In contrast, three non-reactive NADPH-dependent metabolites were formed from PK **13** (Fig. 6B); the accurate mass measurement of 183.1017 corresponds to hydroxylated (M + 16) PK **13** metabolites (δ p.p.m. 0.71). In separate experiments attempting to trap and identify also the generated reactive cytotoxic metabolites (data not shown), inclusion of NAC and NAL in the metabolic incubations resulted in additional chromatographic peaks with both substrates that were tentatively identified as the NAC/NAL adducts of the cytotoxic metabolites (Supplementary Figure S3) (Baer *et al.*, 2005).

Discussion

Human native CYP4B1 is considered to be an orphan P450 since the enzyme cannot bioactivate 4-IPO **12**, the typical substrate for all animal CYP4B1 isoforms, due to the proline-to-serine substitution on position 427 within the highly conserved meander region (Zheng *et al.*, 1998). Therefore, 4-IPO **12** was thought to be an ideal candidate pro-drug for a suicide gene system with an active CYP4B1 enzyme to be used as a safety mechanism in cellular therapies with genetically modified cells. The first attempt used the highly active rabbit CYP4B1 enzyme in combination with 4-IPO **12** and 2-AA **20** as pro-drugs (Rainov *et al.*, 1998); however, *in vivo* testing of this combination was not possible as no knockout animal model was available prior to generating the *Cyp4b1-/-* mouse (Parkinson *et al.*, 2013). In order to reduce the risk of immunogenicity when using a CYP4B1-based suicide gene system, we have rendered the native *human* enzyme capable of metabolizing 4-IPO **12** by changing 13 single amino acids to residues present in the rabbit CYP4B1 isoform and also in other human CYP4 family members at corresponding positions (Wiek *et al.*, 2015). In a next step, we optimized the lentiviral expression vector for the clinical application and identified a more potent pro-drug for T-cell inactivation, namely PK **13** (Roellecke *et al.*, 2016). Therefore, our considerable efforts have resulted in the *re-design* of human CYP4B1 toward a highly active bioactivating enzyme as gauged by cytotoxicity toward 4-IPO **12** in human whole cell systems.

In the present study, we wanted to better understand characteristics of substrates that can be processed/bioactivated by the different CYP4B1 isoforms and also to seek new alternative substrates as potential pro-drugs/toxins for use with the re-engineered human CYP4B1 enzyme. To this end, a library of structurally related substrates was initially tested for cytotoxic activity in human liver-derived cells with an optimal environment for P450 enzymes. These HepG2 liver cells stably expressed four different CYP4B1 isoforms, the rabbit wild-type r-P422 and human wild-type h-S427, the human activated h-P427 and the human re-engineered h-P + 12 proteins. With the selected target compounds, survival of HepG2 cells expressing the different CYP4B1 isoforms was assessed after 24 and 48 h of continuous exposure, using a flow cytometry-based live/dead

readout system. Three compounds, namely 4-IPO **12**, PK **13** and 2-AA **20**, exhibited strong and comparable specific cytotoxicity in HepG2 cells expressing the three *active* CYP4B1s (r-P422, h-P427 or h-P + 12), while non-transduced cells and cells transduced with the control vector or the human h-S427 cDNA did not show any cell death when exposed to increasing drug concentrations up to 290 µM for up to 48 h. Although almost indistinguishable in the bioactivation of these three toxins, there was a clear difference between the rabbit and the two active human enzymes for 2-FPK **14**, 2-PenF **15** and 2-HexF **16**. While the rabbit r-P422 protein converted these three substrates quite efficiently to cytotoxic metabolites, the h-P427 isoform was much less active and the h-P + 12 almost inactive, thus demonstrating that significant differences in the substrate specificities between the CYP4B1 enzymes exist. At lower concentrations, incubation of the cells with 3-MI **18** induced specific cell death through processing by r-P422 and h-P + 12 but not h-P427. At higher concentrations of 3-MI **18**, nonspecific toxicities were observed in all cells, including the control cells. Finally, incubation of the cells with 2-HepF **17** and 2-AF **19** revealed no specific toxicity, although our biochemical studies revealed that at least 2-HepF **17** was efficiently depleted by all purified enzymes to almost the same extent.

As established parameters for the enzymatic activity, we additionally tested the ligand binding affinities and the *in vitro* substrate depletion of the newly identified substrates (2-FPK **14**, 2-HexF **16** and 2-HepF **17**) in comparison to 4-IPO **12** and PK **13** with purified CYP4B1 isoforms. These latter efforts required optimal expression in bacteria and purification of the different CYP4B1 isoforms. It is widely recognized, *inter alia* for eukaryotic P450s and CPRs, that membrane-bound regions can severely reduce the yield of heterologous protein in *E. coli* (Purnapatre *et al.*, 2008; Zelasko *et al.*, 2013). Here, the idea is that the hydrophobicity of the N-terminal anchor of these enzymes and the absence of an inner membrane system impede efficient expression. Thus, one approach is to modify or truncate the N-terminal sequence to a greater or lesser extent. This strategy has worked well in some instances, for example for bacterial expression of the CPRs from *Saccharomyces cerevisiae* (Lamb *et al.*, 2001) and *Candida apicola* (Girhard *et al.*, 2013). For recombinant protein expression in *E. coli*, Cheesman *et al.* (2003) previously demonstrated the successful deletion and substitution/modification of the N-terminus of rabbit CYP4B1. We wanted to reproduce this work with the human activated h-P427 and re-engineered h-P + 12 using r-P422 to establish the expression and purification steps. With our altered processes for protein isolation and purification, we were able to produce up to 800 nmol·l^{-1} of functional r-P422 enzyme. Surprisingly, the straightforward approach applying the same N-terminal MALLLAVF-modification and MA-modification/truncation to h-P427 did not lead to any functional P450 in the soluble fraction. Here, only the deletion of additional amino acids (Δ3-truncation) led to 20–50 nmol·l^{-1}. For h-P + 12, up to 68 nmol·l^{-1} protein could be generated with the Δ3-truncation. Clearly, the expression levels were higher when the sequence of the human protein was more similar to that of the rabbit protein. Quite unexpectedly, however, in some cases the expression levels were also higher with the rather unusual combination of the pCWOri vector and C43(DE3), where the latter host strain was used instead of DH5αF'I^q. Our bacterial expression results confirmed previous observations that there is no general rule that allows prediction of the yields of recombinant mammalian P450s in *E. coli* beforehand; instead an empirical approach of employing several (including 'unusual') combinations of both vectors and host cells was better suited to obtain optimal results.

Gratifyingly, the purified and reconstituted r-P422 and h-P + 12 enzymes displayed the same tendencies when the K_D values and conversions of 4-IPO **12** and PK **13** were compared across enzymes. The slightly different K_D values of h-P427 in comparison to h-P + 12 as well as the differences in the extent of substrate depletion likely reflect the influence of the substituted amino acids on the substrate binding loops (Wiek *et al.*, 2015). Overall, the observed behavior of recombinant r-P422, h-P427 and h-P + 12 in the *in vitro* reactions correspond very well with the results obtained with the cytotoxicity assays employing HepG2 cells, especially when the diversity of these methods is considered.

Most interestingly, major differences were observed in the ligand binding and metabolic conversion of 4-IPO **12** compared to PK **13**, for any given enzyme studied. These two substrates differ only in the hydrophobicity of the terminal portion of their alkyl chains, where a methyl group in PK **13** replaces a hydroxyl group in 4-IPO **12**. This results in very substantially increased metabolic conversion of PK **13** by r-P422, to the extent that almost all of this substrate was depleted over an incubation period of 30 min. The active sites of most P450s are quite hydrophobic and an evaluation of the spectrum of substrates known for r-P422 suggested that this is also true for CYP4B1 (Fisher *et al.*, 1998; Henne *et al.*, 2001a,b). Our preliminary identification studies indicate that non-reactive hydroxylated products are the major oxidative metabolites of PK **13**, but not of 4-IPO **12** (Supplementary Figure S3). We therefore hypothesize that, in contrast to 4-IPO **12**, PK **13** can enter the active site of CYP4B1 in two different binding orientations: the first binding orientation results in non-reactive reaction products through hydroxylation of a carbon atom of the alkyl chain in three possible positions (as confirmed by MS analysis), while the second binding orientation results in (an) reactive enedial intermediate(s) through epoxidation of the furan ring and subsequent rearrangement reactions similar to the bioactivation of 4-IPO **12** (Baer *et al.*, 2005) (as suggested by preliminary results from 'trapping-experiments' with NAC/NAL). However, this alternative pathway does not diminish the cytotoxicity of PK **13** compared to 4-IPO **12** in whole cells, where glucuronidation of 4-IPO **12** is presumably the dominant inactivation route (Parkinson *et al.*, 2016). Conceivably, initially hydroxylated metabolites of PK **13**, might also serve as CYP4B1 substrates and be bioactivated on the furan ring in a second oxidative step (Supplementary Figure S3), but this remains to be determined.

In summary, the establishment of the recombinant expression of human CYP4B1 isoforms in human cells and *E. coli* paves the way for further biochemical and pharmacological characterization of the substrate specificity of CYP4B1 and might shed more light on the evolutionary surprising complete inactivation of CYP4B1 in *Homo sapiens*. Our data also adds valuable contributions to the establishment of *human* CYP4B1 as suicide gene for adoptive cellular therapy in humans.

Supplementary data

Supplementary data are available at *Protein Engineering, Design & Selection* online.

Acknowledgements

We would like to thank Ralf Einholz (Institute of Organic Chemistry, University of Tübingen, Germany) for synthesis of PK **13**, Sebastian Hölzel (Institute of Biochemistry, Heinrich-Heine University Düsseldorf) for technical

assistance and Jörg Schipper (Düsseldorf, Germany) for supporting our research efforts.

Funding

This work was initially supported by the National Institutes of Health [grant number R01 GM49054 to A.E.R.] and subsequently by the UW School of Pharmacy Brady Fund for Natural Products Research [to A.E.R.]; the National Institutes of Health [training grant number T32 GM07750 to J.P. K.]; the Forschungskommission of the Medical Faculty [grant number 39/2012 to C.W.] and the Strategic Research Fund of the Heinrich-Heine University Düsseldorf, Germany [to C.W. and M.G.], as well as the Deutsche Jose Carreras Leukämie-Stiftung e.V. [grant number DJCLS R15/10 to H.H.].

References

Baer,B.R. and Rettie,A.E. (2006) *Drug Metab. Rev.*, **38**, 451–476. doi:10.1080/03602530600688503.

Baer,B.R., Rettie,A.E. and Henne,K.R. (2005) *Chem. Res. Toxicol.*, **18**, 855–864. doi:10.1021/tx0496993.

Barnes,H.J. (1996) *Methods Enzymol.*, **272**, 3–14. doi:10.1016/S0076-6879(96)72003-7.

Barnes,H.J., Arlotto,M.P. and Waterman,M.R. (1991) *Proc. Natl. Acad. Sci. USA*, **88**, 5597–5601. doi:10.1073/pnas.88.13.5597.

Boyd,M.R. (1976) *Environ. Health Perspect.*, **16**, 127–138.

Bradford,M.M. (1976) *Anal. Biochem.*, **72**, 248–254. doi:10.1016/0003-2697(76)90527-3.

Breeze,R.G., Legreid,W.W., Bayly,W.M. and Wilson,B.J. (1984) *Equine. Vet. J.*, **16**, 180–184. doi:10.1111/j.2042-3306.1984.tb01897.x.

Cheesman,M.J., Baer,B.R., Zheng,Y.M., Gillam,E.M. and Rettie,A.E. (2003) *Arch. Biochem. Biophys.*, **416**, 17–24. doi:10.1016/S0003-9861(03)00278-9.

Chen,L.J., DeRose,E.F. and Burka,L.T. (2006) *Chem. Res. Toxicol.*, **19**, 1320–1329. doi:10.1021/tx060128f.

Edson,K.Z. and Rettie,A.E. (2013) *Curr. Top. Med. Chem.*, **13**, 1429–1440. doi:10.2174/15680266113139990110.

Falzon,M., McMahon,J.B., Schuller,H.M. and Boyd,M.R. (1986) *Cancer. Res.*, **46**, 3484–3489.

Fisher,M.B., Zheng,Y.M. and Rettie,A.E. (1998) *Biochem. Biophys. Res. Commun.*, **248**, 352–355. doi:10.1006/bbrc.1998.8842.

Garst,J.E., Wilson,W.C., Kristensen,N.C., Harrison,P.C., Corbin,J.E., Simon, J., Philpot,R.M. and Szabo,R.R. (1985) *J. Anim. Sci.*, **60**, 248–257. doi:10.2527/jas1985.601248x.

Girhard,M., Klaus,T., Khatri,Y., Bernhardt,R. and Urlacher,V.B. (2010) *Appl. Microbiol. Biotechnol.*, **87**, 595–607. doi:10.1007/s00253-010-2472-z.

Girhard,M., Tieves,F., Weber,E., Smit,M.S. and Urlacher,V.B. (2013) *Appl. Microbiol. Biotechnol.*, **97**, 1625–1635. doi:10.1007/s00253-012-4026-z.

Greco,W.R. and Hakala,M.T. (1979) *J. Biol. Chem.*, **254**, 12104–12109.

Hasler,J.A., Estabrook,R., Murray,M., *et al.* (1999) *Mol. Aspects Med.*, **20**, 1–137. doi:10.1016/S0098-2997(99)00005-9.

Henne,K.R., Fisher,M.B., Iyer,K.R., Lang,D.H., Trager,W.F. and Rettie,A.E. (2001a) *Biochemistry*, **40**, 8597–8605. doi:10.1021/bi010395e.

Henne,K.R., Kunze,K.L., Zheng,Y.M., Christmas,P., Soberman,R.J. and Rettie, A.E. (2001b) *Biochemistry*, **40**, 12925–12931. doi:10.1021/bi011171z.

Imaoka,S., Hayashi,K., Hiroi,T., Yabusaki,Y., Kamataki,T. and Funae,Y. (2001) *Biochem. Biophys. Res. Commun.*, **284**, 757–762. doi:10.1006/bbrc.2001.5055.

Isin,E.M. and Guengerich,F.P. (2008) *Anal. Bioanal. Chem.*, **392**, 1019–1030. doi:10.1007/s00216-008-2244-0.

Jang,S.J., Kang,J.H., Lee,T.S., Kim,S.J., Kim,K.I., Lee,Y.J., Cheon,G.J., Choi, C.W. and Lim,S.M. (2010) *Nucl. Med. Mol. Imaging*, **44**, 193–198. doi:10.1007/s13139-010-0038-8.

Jefcoate,C.R. (1978) *Methods Enzymol.*, **52**, 258–279.

Karjoo,Z., Chen,X. and Hatefi,A. (2016) *Adv. Drug Deliv. Rev.*, **99**, 113–128. doi:10.1016/j.addr.2015.05.009.

Kasturi,V.K., Dearing,M.P., Piscitelli,S.C., *et al.* (1998) *Clin. Cancer Res.*, **4**, 2095–2102.

Kerr,L.A., Johnson,B.J. and Burrows,G.E. (1986) *Vet. Hum. Toxicol.*, **28**, 412–416.

Khatri,Y., Girhard,M., Romankiewicz,A., Ringle,M., Hannemann,F., Urlacher,V.B., Hutter,M.C. and Bernhardt,R. (2010) *Appl. Microbiol. Biotechnol.*, **88**, 485–495. doi:10.1007/s00253-010-2756-3.

Khatri,Y., Hannemann,F., Girhard,M., Kappl,R., Hutter,M., Urlacher,V.B. and Bernhardt,R. (2015) *FEBS J.*, **282**, 74–88. doi:10.1111/febs.13104.

Lakhanpal,S., Donehower,R.C. and Rowinsky,E.K. (2001) *Invest. New Drugs*, **19**, 69–76. doi:10.1023/A:1006408803734.

Lamb,D.C., Warrilow,A.G., Venkateswarlu,K., Kelly,D.E. and Kelly,S.L. (2001) *Biochem. Biophys. Res. Commun.*, **286**, 48–54. doi:10.1006/bbrc.2001.5338.

Matsuura,T. (1957) *Bull. Chem. Soc. Jpn*, **30**, 430,431.

Mohr,L., Rainov,N.G., Mohr,U.G. and Wands,J.R. (2000) *Cancer Gene. Ther.*, **7**, 1008–1014. doi:10.1038/sj.cgt.7700190.

Omura,T. and Sato,R. (1964) *J. Biol. Chem.*, **239**, 2379–2385.

Ortiz De Montellano,P.R. (2008) *Drug Metab. Rev.*, **40**, 405–426. doi:10.1080/03602530802186439.

Parkinson,O.T., Liggitt,H.D., Rettie,A.E. and Kelly,E.J. (2013) *Toxicol. Sci.*, **134**, 243–250. doi:10.1093/toxsci/kft123.

Parkinson,O.T., Teitelbaum,A.M., Whittington,D., Kelly,E.J. and Rettie,A.E. (2016) *Drug Metab. Dispos.*, **44**, 1598–1602. doi:10.1124/dmd.116.070003.

Purnapatre,K., Khattar,S.K. and Saini,K.S. (2008) *Cancer Lett.*, **259**, 1–15. doi:10.1016/j.canlet.2007.10.024.

Rainov,N.G. (2000) *Hum. Gene. Ther.*, **11**, 2389–2401. doi:10.1089/104303400750038499.

Rainov,N.G., Dobberstein,K.U., Sena-Esteves,M., Herrlinger,U., Kramm,C. M., Philpot,R.M., Hilton,J., Chiocca,E.A. and Breakefield,X.O. (1998) *Hum. Gene. Ther.*, **9**, 1261–1273. doi:10.1089/hum.1998.9.9-1261.

Ramakanth,S., Thornton-Manning,J.R., Wang,H., Maxwell,H. and Yost,G.S. (1994) *Toxicol. Lett.*, **71**, 77–85. doi:10.1016/0378-4274(94)90201-1.

Robertson,I.G., Serabjit-Singh,C., Croft,J.E. and Philpot,R.M. (1983) *Mol. Pharmacol.*, **24**, 156–162.

Roellecke,K., Virts,E.L., Einholz,R., *et al.* (2016) *Gene. Ther.*. doi:10.1038/gt.2016.38.

Rowinsky,E.K., Chaudhry,V., Forastiere,A.A., Sartorius,S.E., Ettinger,D.S., Grochow,L.B., Lubejko,B.G., Cornblath,D.R. and Donehower,R.C. (1993) *J. Clin. Oncol.*, **11**, 2010–2020.

Schenkman,J.B., Sligar,S.G. and Cinti,D.L. (1981) *Pharmacol. Ther.*, **12**, 43–71. doi:10.1016/0163-7258(81)90075-9.

Schmidt,E.M., Wiek,C., Parkinson,O.T., *et al.* (2015) *PLoS ONE*, **10**, e0137110. doi:10.1371/journal.pone.0137110.

Smith,P.B., Tiano,H.F., Nesnow,S., Boyd,M.R., Philpot,R.M. and Langenbach,R. (1995) *Biochem. Pharmacol.*, **50**, 1567–1575. doi:10.1016/0006-2952(95)02029-2.

Thornton-Manning,J., Appleton,M.L., Gonzalez,F.J. and Yost,G.S. (1996) *J. Pharmacol. Exp. Ther.*, **276**, 21–29.

Vanderslice,R.R., Philpot,R.M., Boyd,J.A. and Eling,T.E. (1985) *Cancer Res.*, **45**, 5851–5858.

Verschoyle,R.D., Philpot,R.M., Wolf,C.R. and Dinsdale,D. (1993) *Toxicol. Appl. Pharmacol.*, **123**, 193–198. doi:10.1006/taap.1993.1237.

Wiek,C., Schmidt,E.M., Roellecke,K., *et al.* (2015) *Biochem. J.*, **465**, 103–114. doi:10.1002/jcc.20084.

Wu,Z.L., Qiao,J., Zhang,Z.G., Guengerich,F.P., Liu,Y. and Pei,X.Q. (2009) *Biotechnol. Lett.*, **31**, 1589–1593. doi:10.1007/s10529-009-0059-5.

Yost,G.S. (1989) *Chem. Res. Toxicol.*, **2**, 273–279.

Zelasko,S., Palaria,A. and Das,A. (2013) *Protein Expr. Purif.*, **92**, 77–87. doi:10.1016/j.pep.2013.07.017.

Zhang,J.Y., Wang,Y. and Prakash,C. (2006) *Curr. Drug Metab.*, **7**, 939–948. doi:10.2174/138920006779010575.

Zheng,Y.M., Baer,B.R., Kneller,M.B., Henne,K.R., Kunze,K.L. and Rettie,A.E. (2003) *Biochemistry*, **42**, 4601–4606. doi:10.1021/bi020667t.

Zheng,Y.M., Fisher,M.B., Yokotani,N., Fujii-Kuriyama,Y. and Rettie,A.E. (1998) *Biochemistry*, **37**, 12847–12851. doi:10.1021/bi981280m.